Letter

Isomeric structure in the ^{100}Sn region: Possible competition between β^+ decay and proton emission in the isomeric unbound nucleus ^{97}Sn

Boshuai Cai,[1] Cenxi Yuan,[1,*] Guangxin Zhang,[1] Yinu Zhang,[1] Menglan Liu,[1] Yuanming Xing,[2] Xinxing Xu,[2] Jianguo Li,[2] and Meng Wang[2]

[1]*Sino-French Institute of Nuclear Engineering and Technology, Sun Yat-sen University, Zhuhai 519082, China*

[2]*Key Laboratory of High Precision Nuclear Spectroscopy and Center for Nuclear Matter Science, Institute of Modern Physics, Chinese Academy of Sciences, Lanzhou 730000, China*

(Received 27 February 2024; accepted 19 April 2024; published 9 May 2024)

The isomeric structure and properties in proton-rich nuclides are crucial for determining the path of the rapid proton capture process (rp-process). For example, bound nuclei inside the dripline can have unbound isomeric states and change the rp-process pathway. The configuration interaction shell model is used to investigate nuclei around the $Z = N$ line at the southwest region of ^{100}Sn. The excitation mechanism of $1/2^-_1$ isomers is identified as dominated by exciting one nucleon in the $1p_{1/2}$ orbit to the $0g_{9/2}$ orbit. The study explores the decay properties of both the ground and isomeric states. Remarkably, competitive β^+ decay and proton emission are predicted in the unbound $1/2^-_1$ isomer of ^{97}Sn, suggesting potential influences on the rp-process pathway.

DOI: 10.1103/PhysRevC.109.L051302

The boundaries of the nuclear landscape [1] and the origins of heavy elements [2] stand as pivotal inquiries within the realms of nuclear physics and astronomy. Both inquiries are intricately connected to the rapid proton capture process (rp-process), a phenomenon integral to the creation of proton-rich nuclides, spanning from CNO cycles to SnSbTe cycles [3].

The rp-process trajectory unfolds as a consequence of the interplay between proton capture, proton emission, and β^+ decay. Crucial to understanding this process are the ground-state properties of proton-rich nuclides, especially nuclear mass and the partial half-lives of β^+ decay and proton emission [4–6]. The precise measurement or prediction of these properties significantly influences the identification of waiting points [7–10] and ending points [11–14] in the rp-process.

When a captured proton is weakly bound or unbound, its removal becomes facile [10]. Subsequently, slow β^+ decay predominates at waiting points, and the daughter nucleus readies itself for the subsequent proton capture [15]. Since isomers will be produced after proton capture and β^+ decay, their excitation energy and decay properties are thus also of particular importance to the rp-process [3,6]. These exotic isomers possess the potential to alter the rp-process trajectory [16] and influence the abundance of p-nuclides in the universe. For example, a nuclide, whose ground state is proton bound but whose isomer is proton unbound, may change its waiting point characteristic.

Similar cases have been observed in the s-process and the r-process. The 305-keV $1/2^-$ isomer of ^{85}Kr, with a β^- decay half-life of 4.5 h, favors β^- decay over neutron capture at low temperature, altering its branching-point characteristic in the s-process [17]. The isomers of ^{128}Sb, with a shorter half-life of β^- decay than its ground state, accelerate abundance evolution and energy release in the r-process [18,19]. Therefore, high-precision excitation energy, the corresponding excitation mechanism, and decay properties of isomers in proton-rich nuclides are imperative to enhance the understanding of the rp-process [4] and comprehend the role of isomers in nucleosynthesis [19].

The southwestern region of ^{100}Sn, specifically the upper p_1g_9 shell, holds a distinctive status regarding low-lying $1/2^-_1$ isomers. The ground states of these odd-mass nuclides are predominantly influenced by an unpaired nucleon in the $0g_{9/2}$ orbit, while the $1/2^-_1$ isomers primarily arise from an unpaired nucleon occupying the $1p_{1/2}$ orbit. Recent measurements of the excitation energies of $1/2^-_1$ isomers in ^{99}In [20] and ^{95}Pd [21] provide additional insights into $1/2^-_1$ isomers induced by unpaired protons (neutrons), contributing to a more systematic analysis of the excitation mechanisms.

This Letter delves into the investigation of the excitation mechanism of these $1/2^-_1$ isomers and explores the competition between proton emission and β^+ decay in both the ground and isomeric states.

The monopole-based universal interaction V_{MU} [22], incorporating a Gaussian-type central force and a $\pi + \rho$ tensor force [23], in conjunction with the spin-orbit force M3Y [24], serves as the foundation for generating configuration interaction shell model (CISM) Hamiltonians within the f_5pg_9 model space. The mass dependence [25] is also implemented. The weakly bound effect (WBE), which aptly describes the large mirror energy difference (MED) around $A = 20$ [26–29] and the isospin mixing in ^{26}Si [30], may play a role in elucidating these $1/2^-_1$ isomers in the upper p_1g_9 shell. The WBE broadens the proton single-particle wave function in coordinate

*yuancx@mail.sysu.edu.cn

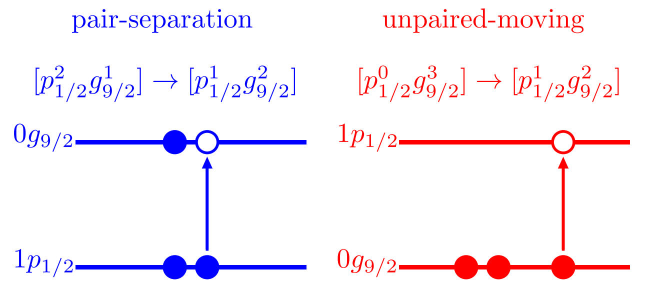

FIG. 1. Illustration of the pair-separation and unpaired-moving mechanisms of exciting $9/2^+_1$ to $1/2^-_1$ in ^{91}Nb.

space, leading to a reduction of the two-body matrix elements (TBME) [28,29]. Given that the proton dripline lies alongside the $Z = N$ line in the upper p_1g_9 shell [15], and the p orbit experiences low centrifugal potential, the $1/2^-_1$ isomers in this region involving the proton $1p_{1/2}$ orbit may be influenced by the WBE. To address the WBE in the present Letter, a factor, denoted as $\lambda_{\pi p_{1/2}}$, is introduced for the proton $1p_{1/2}$ orbit and subsequently applied to the associated TBME. For instance, the TBME $\langle \pi p_{1/2}\pi p_{1/2}|V|\pi g_{9/2}\pi g_{9/2}\rangle_J$ is scaled by $\lambda^2_{\pi p_{1/2}}$. The excitation energies of the low-lying $1/2^-_1$ of $N = 50$ and $N = 49$ odd-A nuclides with $Z \geqslant 40$, i.e., ^{91}Nb, ^{93}Tc, ^{95}Rh, ^{97}Ag, ^{99}In, ^{89}Zr, ^{91}Mo, ^{93}Ru, and ^{95}Pd, are employed to refine $\lambda_{\pi p_{1/2}}$, along with the proton and neutron $1p_{1/2}$ single-particle energies. Analogous corrections are implemented in the light nuclei, well describing the MED [28,29]. The large-scale CISM calculations are carried out using the KSHELL code [31,32].

The southwest corner of ^{100}Sn is a region where the $1/2^-_1$ isomers of odd-A nuclides are systematically observed. Two mechanisms of exciting $9/2^+_1$ to $1/2^-_1$ may be feasible depending on the Z $(N) = 40$ subshell. As depicted in Fig. 1 for the proton isomer of ^{91}Nb, one can either separate the proton pair in the $1p_{1/2}$ orbit and excite one of them to the $0g_{9/2}$ orbit (pair-separation) or move an unpaired proton in the $0g_{9/2}$ orbit to the $1p_{1/2}$ orbit (unpaired-moving). The evolution of the energy difference between $1/2^-_1$ and $9/2^+_1$ aids in understanding the mechanism to form the isomers.

The experimental $E_x(1/2^-_1)-E_x(9/2^+_1)$ of odd-A nuclides increases with the proton number in the isotonic chains, as shown in Fig. 2. The interaction of the present work and the JUN45 interaction [25] is used to perform the CISM calculation. Results of the former interaction are consistent with the experimental values, while those of the latter present a parabolic evolution of $E_x(1/2^-_1)-E_x(9/2^+_1)$ in $N = 50$ isotones, caused by the competition between different excitation mechanisms.

To investigate this further, the $1/2^-_1$ state of $N = 50$ isotones is assumed with only one proton in the $1p_{1/2}$ orbit, and the $9/2^+_1$ state is assumed with pair-separation and unpaired-moving configurations, respectively, in Fig. 2. Since the unpaired-moving configuration is forbidden for ^{99}In$(9/2^+_1)$ in the f_5pg_9 model space, the excitation energy of the two mechanisms is shifted to align at ^{99}In. The excitation energy of the pair-separation mechanism increases with the proton number, consistent with the experimental values, while that of the unpaired-moving mechanism exhibits an inverse trend. The excitation from $9/2^+_1$ to $1/2^-_1$ in $N = 50$ isotones is dominated by the pair-separation mechanism.

As of now, the $1/2^-_1$ isomers in the upper p_1g_9 shell have been exclusively measured for nuclides with $Z < N$ [20,21]. These nuclides, characterized by $Z - N = -1$ and -3 with $N \geqslant 45$, lie on the path of the rp-process [33]. Generally, their ground states decay through β^+ decay and β-delayed proton emission, impacting the nucleosynthesis of the rp-process [34]. Due to their S_p and S_{2p} generally exceeding 900 keV [35,36], the $1/2^-_1$ isomers have excitation energies insufficient for proton emission. Corresponding data are listed in Appendix.

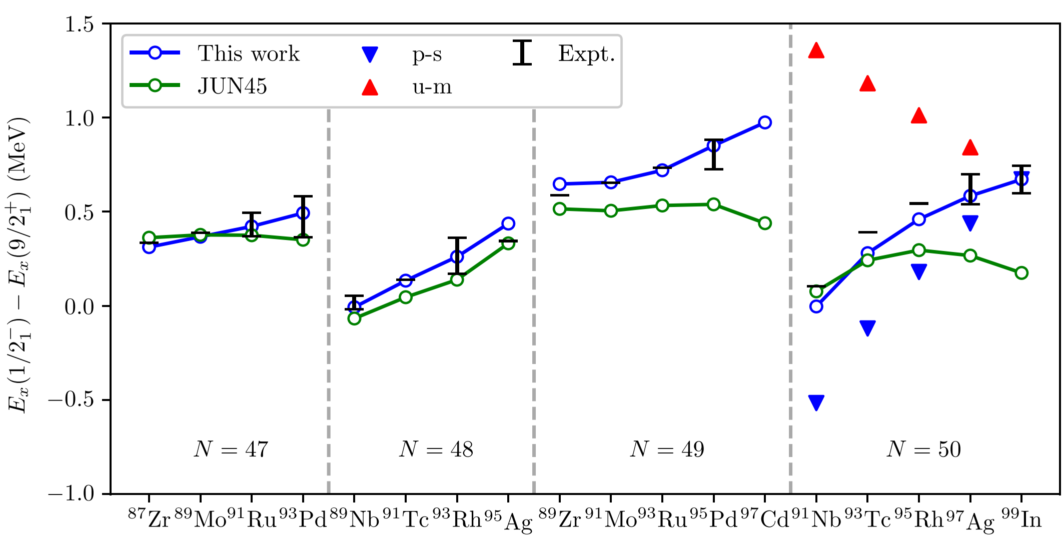

FIG. 2. Energy difference between $1/2^-_1$ and $9/2^+_1$ of $N = 47$, 48, 49, and 50 odd-A nuclides. The up-to-date experimental values are taken from Refs. [20,21] and the National Nuclear Data Center (NNDC) [38]. p-s (u-m) denotes that the $9/2^+_1$ state is assumed with the pair-separation (unpaired-moving) configuration. The error bar for experimental values takes $2\sigma_{\rm expt}$.

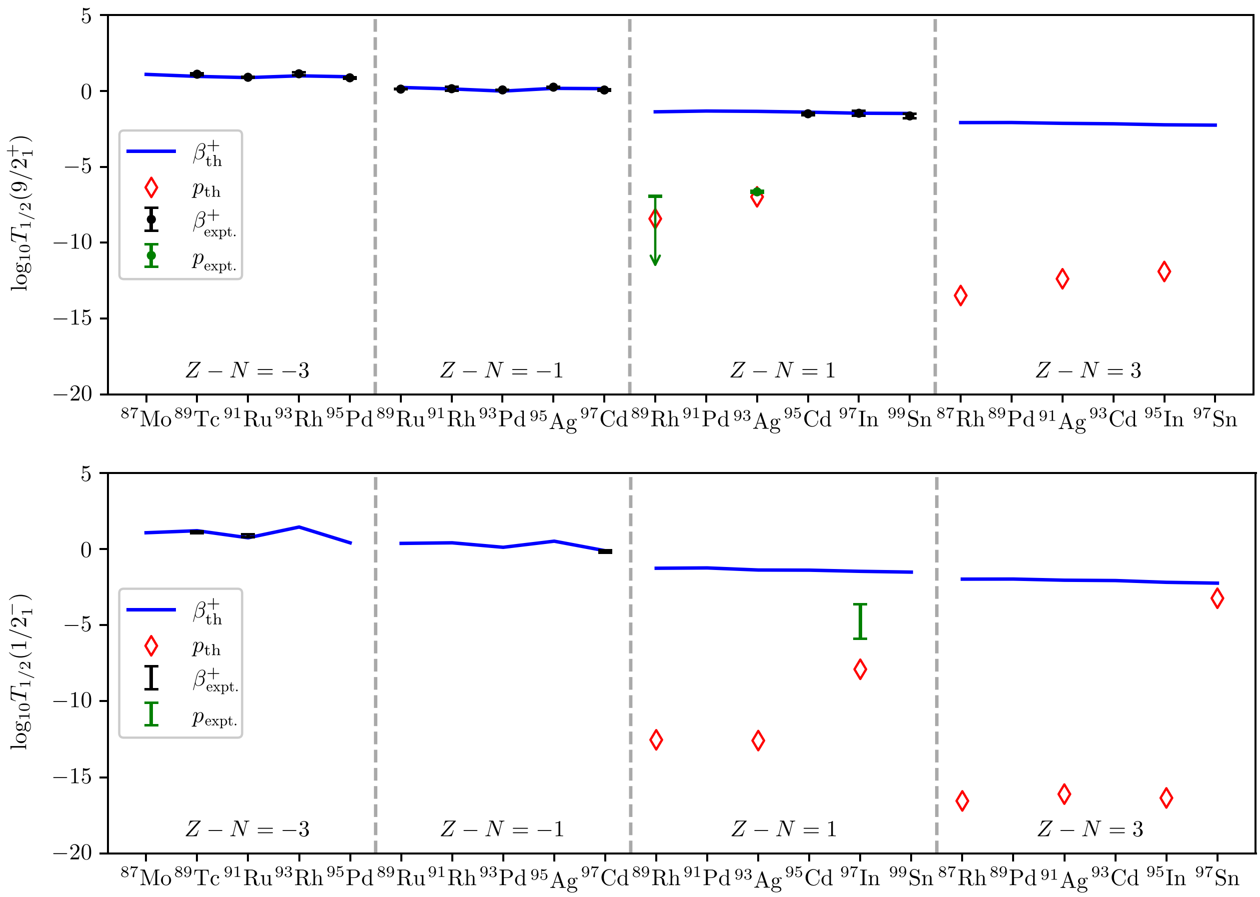

FIG. 3. Half-lives of β^+ decay and proton emission in $9/2_1^+$ and $1/2_1^-$ of $Z-N=\pm1$ and ±3 nuclides. The experimental data are taken from Refs. [37,39–41].

In the case of $Z-N=1$ nuclides, single-proton emission is predicted to be energetically allowed for odd-Z nuclides such as ^{93}Ag and ^{89}Rh, and presumably for their $1/2_1^-$ isomers. ^{97}In is an exception, with its S_p estimated to be -0.10 ± 0.19 MeV by the experimental half-life analysis [37], indicating weak proton emission from the ground state compared with β^+ decay. Nonetheless, proton emission from its $1/2_1^-$ isomer has been detected, with a measured half-life ranging between 1.3 and 230 μs [37]. For even-Z nuclides in this category, such as ^{99}Sn, ^{95}Cd, and ^{91}Pd, both the ground state and the $1/2_1^-$ isomer are bound against single-proton and two-proton emission.

In the case of $Z-N=3$ nuclides, single-proton emission is energetically forbidden for even-Z nuclides but allowable for odd-Z nuclides. Though two-proton emission is energetically allowed for both even-Z and odd-Z nuclides, the diproton emission is weak due to the small value of S_{2p}, which is not further discussed in the present work. ^{97}Sn, with a predicted S_p of 0.199 MeV [35], is intriguing. Here, its $E_x(1/2_1^-)$ is predicted to be 0.911 MeV, rendering it proton unbound. Given that the β^+ decay is a general decay mode of nuclides beyond the stability line, and the large angular momentum difference should hinder the transition from $1/2_1^-$ to $9/2_1^+$, a comprehensive comparison between single-proton emission and β^+ decay in the ground state and the $1/2_1^-$ isomer of these nuclides is therefore essential.

To assess the competition between β^+ decay and proton emission, their partial half-lives are calculated. The proton decay half-life is computed using

$$\frac{\hbar}{\sum_c \theta_c^2\Gamma_c}, \tag{1}$$

where c denotes the proton decay channels, incorporating the initial state, the final state, the orbit of the emitted proton, and the decay energy. Here, θ_c^2 is the CISM spectroscopic factor of channel c, and Γ_c is the decay width of emitting proton through channel c. The WKB approximation [42] is employed to calculate Γ_c, with the mean field characterized by the Chepurnov-parametrized Woods-Saxon potential, the Coulomb interaction, and the centrifugal potential. The β^+ decay half-life is determined by

$$\frac{\kappa}{\sum_b f_0\left[\left(\frac{g_A}{g_V}\right)^2 B_{\rm GT}+B_{\rm F}\right]}, \tag{2}$$

where b represents the channels of β^+ decay from a given initial state, $\kappa=6147$ s, f_0 is the phase-space factor, $g_{A(V)}=1.25$ (1.00) is the axial-vector (vector)-coupling factor, and

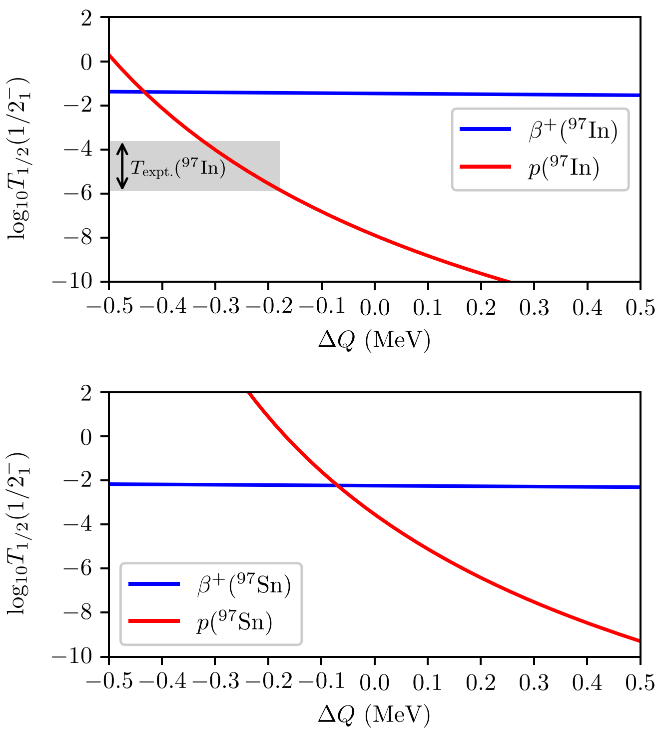

FIG. 4. Half-lives of β^+ decay and proton emission in the $1/2_1^-$ isomers of ^{97}In and ^{97}Sn along the variation of the corresponding decay energy ΔQ. $\Delta Q = 0$ corresponds to half-lives calculated in Fig. 3. The gray region denotes the experimental range of 2.3–130 µs [37] for the proton-emission half-life of ^{97}In.

B_{GT} and B_{F} are the reduced Gamow-Teller and Fermi transition strengths [43]. A standard quenching factor $q^2 = 0.75^2$ is applied for β^+ decay [44–46].

The theoretical partial half-lives are generally in agreement with the experimental values, as shown in Fig. 3. The single-proton dripline in this region was predicted to be reached at $Z - N = 1$ for odd-Z nuclides and extended for even-Z nuclides due to pairing effects [35,36]. Both the ground state and the $1/2_1^-$ isomer of ^{95}In, ^{91}Ag, ^{87}Rh, ^{93}Ag, and ^{89}Rh are predominantly influenced by proton emission, which is expected. For ^{97}In, due to the large uncertainty in S_p, value of -100 keV and $\sigma_{\text{expt}} = 190$ keV [37], the theoretical proton-emission half-life of its $1/2_1^-$ isomer falls outside the experimentally measured range. Taking this into account, the evolution of β^+ decay and proton-emission half-lives of the $1/2_1^-$ isomer of ^{97}In along changes in decay energy is shown in Fig. 4. The β^+ decay half-life is less sensitive to energy compared to proton emission. A decrease by 1 σ_{expt} in decay energy would lead to an increase of proton-emission half-life and make it drop within the experimental range of 1.3–230 µs.

The competition between β^+ decay and proton emission presents an intriguing scenario in ^{97}Sn. Predicted to be proton bound in the ground state, ^{97}Sn is expected to be dominated by β^+ decay, decaying to ^{97}In. However, when considering its $1/2_1^-$ isomer, where proton emission appears, the dynamics shift. The difference in half-lives between β^+ decay and proton emission for this $1/2_1^-$ isomer is approximately 1 order of magnitude. Given the absence of experimental data for ^{97}Sn, the comparable analysis, involving varying decay energy, is conducted for the partial half-lives comparison again. Despite the decay energy decreasing by only 70 keV, β^+ decay becomes competitive with proton emission, introducing two potential decay paths for the $1/2_1^-$ isomer of ^{97}Sn.

While the prevailing notion suggests that the rp-process may not reach ^{97}In [33], the unmeasured masses of nuclides below ^{97}Sn, such as ^{96}In, ^{95}Cd, ^{95}Pd, ^{94}Ag, etc., introduce uncertainties. The pathway contributing to the rp-process for synthesizing ^{95}Cd accounts for over 10% of the maximum reaction flow [33]. Considering these uncertainties of mass and the possibility of $2p$ capture of ^{95}Cd, the reaction flow of the rp-process may indeed extend to ^{97}Sn. Consequently, the $1/2_1^-$ isomer of ^{97}Sn may play a role in the rp process, emphasizing the need for further investigations in rp-process network calculations. The β^+ decay, governed by weak interaction, and the proton emission, driven by electromagnetic and strong interaction, provide a unique perspective to explore the $1/2_1^-$ isomers of ^{97}In and ^{97}Sn. In this context, these isomers provide ideal scenarios for probing the intricate interplay between weak, electromagnetic, and strong interactions, warranting further investigation.

In summary, the CISM has been employed to investigate the $1/2_1^-$ isomers in the upper p_1g_9 shell. The competition between proton emission and β^+ decay of the ground states and $1/2_1^-$ isomers of these $Z - N = 1$ and 3 nuclides has been thoroughly examined. The evolution of $E_x(1/2_1^-)$ has revealed that the dominant excitation mechanism of the $1/2_1^-$ isomer involves taking a pair of nucleons in the $1p_{1/2}$ orbit apart and exciting one of them to the $0g_{9/2}$ orbit. Notably, the $1/2_1^-$ isomer of ^{97}Sn is predicted to exhibit competitive proton emission and β^+ decay. This finding suggests that ^{97}Sn, if produced, may decay through a new path in the rp-process. The accuracy of this prediction relies on precise measurements of the mass and excitation energy of ^{97}Sn. The study emphasizes the intricate interplay between various decay modes in both ground state and isomeric states of exotic nuclei, shedding light on the potential contributions to the rp-process.

This work was supported by the Guangdong Major Project of Basic and Applied Basic Research (Grant No. 2021B0301030006), the Strategic Priority Research Program of Chinese Academy of Sciences (Grant No. XDB34000000), the National Natural Science Foundation of China (Grants No. 12305129, No. 12135017, No. 12121005, No. 12022501, No. 12105329, No. 12205340), the Youth Innovation Promotion Association of Chinese Academy of Sciences (Grant No. 2021419), the Gansu Natural Science Foundation (Grant No. 22JR5RA123), the China Institute of Atomic Energy, the China Nuclear Data Center, and the computational resources from SYSU and the National Supercomputer Center in Guangzhou.

Appendix. Table I list the measured and calculated S_p, S_{2p}, and $E_x(1/2_1^-)$ of nuclides with $Z - N = \pm 3$ and ± 1.

TABLE I. The measured and calculated S_p, S_{2p}, and $E_x(1/2_1^-)$ of nuclides with $Z-N=\pm3$ and ±1. The unit of measure is MeV.

$Z-N$	Nucl.	$S_{p,\mathrm{AME2020}}$ [36]	$S_{p,\mathrm{cal}}$ [35]	$S_{2p,\mathrm{AME2020}}$ [36]	$S_{2p,\mathrm{cal}}$ [35]	$E_{x,\mathrm{exp}}(1/2_1^-)$	$E_{x,\mathrm{cal}}(1/2_1^-)$
−3	^{97}Ag	2.010(13)	2.089	7.141 (13)	7.460	0.620 (40) [21]	0.584
−3	^{95}Pd	4.347(5)	4.489	7.327 (4)	7.566	0.804 (39) [21]	0.851
−3	^{93}Rh	2.000(4)	2.018	7.603 (4)	7.719	0.267 (48) [21]	0.261
−3	^{91}Ru	4.8041(24)	4.824	7.803 (4)	7.851	0.432 (31) [21]	0.422
−3	^{89}Tc	1.997(5)	1.954	8.098 (8)	7.840	0.0626 (5) [38]	0.171
−3	^{87}Mo	5.040(6)	4.747	8.288 (7)	8.183	0.310 (30) [21]	0.285
−1	^{99}In	1.030 (300)[a]	1.207	5.050 (300)[a]	5.657	0.671 (37) [20]	0.672
−1	^{97}Cd	3.510 (430)	3.317	5.350 (420)	5.545	–	0.974
−1	^{95}Ag	1.090 (400)[a]	0.958	5.470 (400)[a]	5.598	0.3442 (3) [38]	0.437
−1	^{93}Pd	3.270 (370)	3.507	5.320 (370)	5.636	0.474 (54) [21]	0.493
−1	^{91}Rh	0.980 (300)[a]	0.851	5.750 (300)[a]	5.716	0.1729 (4) [38]	0.261
−1	^{89}Ru	3.988 (25)	3.509	6.063 (24)	5.613	0.323 (60) [21]	0.341
1	^{99}Sn	1.360 (660)[a]	1.205	1.820 (720)[a]	2.515	–	1.071
1	^{97}In	−0.890 (570)[a]	−1.201	2.060 (570)[a]	2.349	–	0.915
1	^{95}Cd	1.940 (690)[a]	1.076	2.650 (680)[a]	2.605	–	0.553
1	^{93}Ag	−1.090 (530)[a]	−1.119	2.410 (500)[a]	2.568	–	0.419
1	^{91}Pd	1.830 (470)[a]	0.970	2.380 (420)[a]	2.628	–	0.247
1	^{89}Rh	−1.400 (200)[a]	−1.223	2.540 (360)[a]	2.143	–	0.174
3	^{97}Sn	–	0.199	–	−0.735	–	0.911
3	^{95}In	–	−2.215	–	−0.533	–	0.854
3	^{93}Cd	–	0.537	–	−0.367	–	0.374
3	^{91}Ag	–	−2.192	–	−0.381	–	0.400
3	^{89}Pd	–	0.444	–	−0.887	–	0.225
3	^{87}Rh	–	−2.427	–	−1.327	–	0.155

[a]The value is extrapolated based on the trends from the mass surface in AME2020 [36].

[1] J. Erler, N. Birge, M. Kortelainen, W. Nazarewicz, E. Olsen, A. M. Perhac, and M. Stoitsov, Nature (London) **486**, 509 (2012).

[2] S. Sanders, *Science* (AAAS Custom Publishing Office, Washington, DC, 2021).

[3] K. Langanke and M. Wiescher, Rep. Prog. Phys. **64**, 1657 (2001).

[4] H. Schatz, A. Aprahamian, J. Görres, M. Wiescher, T. Rauscher, J. Rembges, F.-K. Thielemann, B. Pfeiffer, P. Möller, K.-L. Kratz, H. Herndl, B. Brown, and H. Rebel, Phys. Rep. **294**, 167 (1998).

[5] H. Schatz, Nucl. Phys. A **251**, 293 (2006).

[6] H. Grawe, K. Langanke, and G. Martínez-Pinedo, Rep. Prog. Phys. **70**, 1525 (2007).

[7] J. J. Ressler, A. Piechaczek, W. B. Walters, A. Aprahamian, M. Wiescher, J. C. Batchelder, C. R. Bingham, D. S. Brenner, T. N. Ginter, C. J. Gross, R. Grzywacz, D. Kulp, B. MacDonald, W. Reviol, J. Rikovska, K. Rykaczewski, J. A. Winger, and E. F. Zganjar, Phys. Rev. Lett. **84**, 2104 (2000).

[8] D. G. Jenkins, Phys. Rev. C **78**, 012801(R) (2008).

[9] A. M. Rogers, M. A. Famiano, W. G. Lynch, M. S. Wallace, F. Amorini, D. Bazin, R. J. Charity, F. Delaunay, R. T. de Souza, J. Elson, A. Gade, D. Galaviz, M.-J. Van Goethem, S. Hudan, J. Lee, S. Lobastov, S. Lukyanov, M. Matoš, M. Mocko, H. Schatz *et al.*, Phys. Rev. Lett. **106**, 252503 (2011).

[10] X. L. Tu, H. S. Xu, M. Wang, Y. H. Zhang, Y. A. Litvinov, Y. Sun, H. Schatz, X. H. Zhou, Y. J. Yuan, J. W. Xia, G. Audi, K. Blaum, C. M. Du, P. Geng, Z. G. Hu, W. X. Huang, S. L. Jin, L. X. Liu, Y. Liu, X. Ma *et al.*, Phys. Rev. Lett. **106**, 112501 (2011).

[11] B. Blank, S. Andriamonje, S. Czajkowski, F. Davi, R. Del Moral, J. P. Dufour, A. Fleury, A. Musquère, M. S. Pravikoff, R. Grzywacz, Z. Janas, M. Pfützner, A. Grewe, A. Heinz, A. Junghans, M. Lewitowicz, J.-E. Sauvestre, and C. Donzaud, Phys. Rev. Lett. **74**, 4611 (1995).

[12] H. Schatz, A. Aprahamian, V. Barnard, L. Bildsten, A. Cumming, M. Ouellette, T. Rauscher, F.-K. Thielemann, and M. Wiescher, Phys. Rev. Lett. **86**, 3471 (2001).

[13] C. Mazzocchi, R. Grzywacz, S. N. Liddick, K. P. Rykaczewski, H. Schatz, J. C. Batchelder, C. R. Bingham, C. J. Gross, J. H. Hamilton, J. K. Hwang, S. Ilyushkin, A. Korgul, W. Królas, K. Li, R. D. Page, D. Simpson, and J. A. Winger, Phys. Rev. Lett. **98**, 212501 (2007).

[14] V.-V. Elomaa, G. K. Vorobjev, A. Kankainen, L. Batist, S. Eliseev, T. Eronen, J. Hakala, A. Jokinen, I. D. Moore, Y. N. Novikov, H. Penttilä, A. Popov, S. Rahaman, J. Rissanen, A. Saastamoinen, H. Schatz, D. M. Seliverstov, C. Weber, and J. Äystö, Phys. Rev. Lett. **102**, 252501 (2009).

[15] M. Pfützner and C. Mazzocchi, in *Handbook of Nuclear Physics*, edited by I. Tanihata, H. Toki, and T. Kajino (Springer Nature, Singapore, 2022), pp. 1–41.

[16] A. Aprahamian and Y. Sun, Nat. Phys. **1**, 81 (2005).

[17] G. W. Misch, S. K. Ghorui, P. Banerjee, Y. Sun, and M. R. Mumpower, Astrophys. J., Suppl. Ser. **252**, 2 (2021).

[18] G. W. Misch, T. M. Sprouse, and M. R. Mumpower, Astrophys. J. Lett. **913**, L2 (2021).

[19] P. M. Walker and Z. Podolyák, Nuclear isomers, in *Handbook of Nuclear Physics*, edited by I. Tanihata, H. Toki, and T. Kajino (Springer Nature, Singapore, 2022), pp. 1–37.

[20] L. Nies, D. Atanasov, M. Athanasakis-Kaklamanakis, M. Au, K. Blaum, J. Dobaczewski, B. S. Hu, J. D. Holt, J. Karthein, I. Kulikov, Y. A. Litvinov, D. Lunney, V. Manea, T. Miyagi, M. Mougeot, L. Schweikhard, A. Schwenk, K. Sieja, and F. Wienholtz, Phys. Rev. Lett. **131**, 022502 (2023).

[21] Y. M. Xing, C. X. Yuan, M. Wang, Y. H. Zhang, X. H. Zhou, Y. A. Litvinov, K. Blaum, H. S. Xu, T. Bao, R. J. Chen, C. Y. Fu, B. S. Gao, W. W. Ge, J. J. He, W. J. Huang, T. Liao, J. G. Li, H. F. Li, S. Litvinov, S. Naimi *et al.*, Phys. Rev. C **107**, 014304 (2023).

[22] T. Otsuka, T. Suzuki, M. Honma, Y. Utsuno, N. Tsunoda, K. Tsukiyama, and M. Hjorth-Jensen, Phys. Rev. Lett. **104**, 012501 (2010).

[23] T. Otsuka, T. Suzuki, R. Fujimoto, H. Grawe, and Y. Akaishi, Phys. Rev. Lett. **95**, 232502 (2005).

[24] G. Bertsch, J. Borysowicz, H. McManus, and W. G. Love, Nucl. Phys. A **284**, 399 (1977).

[25] M. Honma, T. Otsuka, T. Mizusaki, and M. Hjorth-Jensen, Phys. Rev. C **80**, 064323 (2009).

[26] R. G. Thomas, Phys. Rev. **88**, 1109 (1952).

[27] J. B. Ehrman, Phys. Rev. **81**, 412 (1951).

[28] K. Ogawa, H. Nakada, S. Hino, and R. Motegi, Phys. Lett. B **464**, 157 (1999).

[29] C. Yuan, C. Qi, F. Xu, T. Suzuki, and T. Otsuka, Phys. Rev. C **89**, 044327 (2014).

[30] J. Liu, X. Xu, L. Sun, C. Yuan, K. Kaneko, Y. Sun, P. Liang, H. Wu, G. Shi, C. Lin, J. Lee, S. Wang, C. Qi, J. Li, H. Li, L. Xayavong, Z. Li, P. Li, Y. Yang, H. Jian *et al.*, Phys. Rev. Lett. **129**, 242502 (2022).

[31] N. Shimizu, T. Mizusaki, Y. Utsuno, and Y. Tsunoda, Comput. Phys. Commun. **244**, 372 (2019).

[32] N. Shimizu, arXiv:1310.5431.

[33] G. Lorusso, A. Becerril, A. Amthor, T. Baumann, D. Bazin, J. S. Berryman, B. A. Brown, R. H. Cyburt, H. L. Crawford, A. Estrade, A. Gade, T. Ginter, C. J. Guess, M. Hausmann, G. W. Hitt, P. F. Mantica, M. Matos, R. Meharchand, K. Minamisono, F. Montes *et al.*, Phys. Rev. C **86**, 014313 (2012).

[34] R. N. Boyd, in *Proton-Emitting Nuclei: PROCON '99: First International Symposium*, edited by J. C. Batchelder, AIP Conf. Proc. No. 518 (American Institute of Physics, College Park, MD, 2000), p. 239.

[35] B. S. Cai, G. S. Chen, C. X. Yuan, and J. J. He, Chin. Phys. C **46**, 104107 (2022).

[36] M. Wang, W. J. Huang, F. G. Kondev, G. Audi, and S. Naimi, Chin. Phys. C **45**, 030003 (2021).

[37] J. Park, R. Krücken, D. Lubos, R. Gernhäuser, M. Lewitowicz, S. Nishimura, D. S. Ahn, H. Baba, B. Blank, A. Blazhev, P. Boutachkov, F. Browne, I. Čeliković, G. De France, P. Doornenbal, T. Faestermann, Y. Fang, N. Fukuda, J. Giovinazzo, N. Goel *et al.*, Phys. Rev. C **97**, 051301(R) (2018).

[38] National Nuclear Data Center, information extracted from the nudat database, https://www.nndc.bnl.gov/nudat/.

[39] F. G. Kondev, M. Wang, W. J. Huang, S. Naimi, and G. Audi, Chin. Phys. C **45**, 030001 (2021).

[40] J. Park, R. Krücken, D. Lubos, R. Gernhäuser, M. Lewitowicz, S. Nishimura, D. S. Ahn, H. Baba, B. Blank, A. Blazhev, P. Boutachkov, F. Browne, I. Čeliković, G. De France, P. Doornenbal, T. Faestermann, Y. Fang, N. Fukuda, J. Giovinazzo, N. Goel *et al.*, Phys. Rev. C **99**, 034313 (2019).

[41] I. Čeliković, M. Lewitowicz, R. Gernhäuser, R. Krücken, S. Nishimura, H. Sakurai, D. Ahn, H. Baba, B. Blank, A. Blazhev, P. Boutachkov, F. Browne, G. De France, P. Doornenbal, T. Faestermann, Y. Fang, N. Fukuda, J. Giovinazzo, N. Goel, M. Górska *et al.*, Phys. Rev. Lett. **116**, 162501 (2016).

[42] S. Åberg, P. B. Semmes, and W. Nazarewicz, Phys. Rev. C **56**, 1762 (1997).

[43] J. Suhonen, *From Nucleons to Nucleus: Concepts of Microscopic Nuclear Theory* (Springer-Verlag, Berlin, 2007).

[44] A. Mollaebrahimi, C. Hornung, T. Dickel, D. Amanbayev, G. Kripko-Koncz, W. R. Plaß, S. Ayet San Andrés, S. Beck, A. Blazhev, J. Bergmann, H. Geissel, M. Górska, H. Grawe, F. Greiner, E. Haettner, N. Kalantar-Nayestanaki, I. Miskun, F. Nowacki, C. Scheidenberger, S. Bagchi *et al.*, Phys. Lett. B **839**, 137833 (2023).

[45] L. Batist, M. Górska, H. Grawe, Z. Janas, M. Kavatsyuk, M. Karny, R. Kirchner, M. La Commara, I. Mukha, A. Plochocki, and E. Roeckl, Eur. Phys. J. A **46**, 45 (2010).

[46] I. S. Towner, Phys. Rep. **155**, 263 (1987).